Cytoarchitecture, morphology, and lumbosacral spinal cord projections of the red nucleus in cattle

Roberto Chiocchetti, DVM, PhD; Cristiano Bombardi, DVM, PhD; Annamaria Grandis, DVM, PhD; Gemma Mazzuoli, DVM; Arcangelo Gentile, DVM; Luciano Pisoni, DVM; Monica Joechler, DVM; Maria Luisa Lucchi, BS

Objective—To analyze the morphology, cytoarchitecture, and lumbosacral spinal cord projections of the red nucleus (RN) in cattle.

Animals—8 healthy Friesian male calves.

Procedures—Anesthetized calves underwent a dorsal laminectomy at L5. Eight bilateral injections (lateral to the midline) of the neuronal retrograde fluorescent tracer fast blue (FB) were administered into the exposed lumbosacral portion of the spinal cord. A postsurgical calf survival time of 38 to 55 days was used. Following euthanasia, the midbrain and the L5-S2 spinal cord segments were removed. Nissl's method of staining was applied on paraffin-embedded and frozen sections of the midbrain.

Results—The mean length of the RN from the caudal to cranial end ranged from 6,680 to 8,640 μm. The magnocellular and parvicellular components of the RN were intermixed throughout the nucleus, but the former predominate at the caudal portion of the nucleus and the latter at the cranial portion with a gradual transitional zone. The FB-labeled neurons were found along the entire craniocaudal extension of the nucleus, mainly in its ventrolateral part. The number of FB-labeled neurons was determined in 4 calves, ranging from 191 to 1,469 (mean, 465). The mean cross-sectional area of the FB-labeled neurons was approximately 1,680 μm^2.

Conclusions and Clinical Relevance—In cattle, small, medium, and large RN neurons, located along the entire craniocaudal extension of the RN, contribute to the rubrospinal tract reaching the L6-S1 spinal cord segments. Thus, in cattle, as has been shown in cats, the RN parvicellular population also projects to the spinal cord. (*Am J Vet Res* 2006;67:1662–1669)

Abbreviations

RN	Red nucleus
RNm	RN magnocellular region
RNp	RN parvicellular region
LVN	Lateral vestibular nucleus
BSP	Bovine spastic paresis
FB	Fast blue

The RN and the prominent rubrospinal tract are present in all limbed terrestrial vertebrates. The mammalian RN is a well-recognized component of the motor system located in the tegmentum of the cranial half of the midbrain at the level of the oculomotor nerve. A considerable volume of literature exists concerning its morphology, its cytoarchitecture, and its functional connections in a variety of mammals.[1–5] The RN is traditionally subdivided into a caudally located RNm and a cranially located RNp. The RNm receives input mainly from the cerebellar interpositus nucleus and less from lateral nucleus (dentate nucleus) and projects mainly to the contralateral spinal cord[5,6]; the RNp receives input from the cerebellar lateral nucleus and projects to the ipsilateral nucleus olivaris.[6] The RN also seems to be reciprocally connected with the LVN, providing the basis for coordinated activity of both structures during the development of vestibulospinal and rubrospinal motor events.[7,8] Also, connectivity between the divisions of the RN and the cortex has been studied; corticorubral axons projecting mainly from the motor area were mapped in the RNp and in RNm of monkeys.[9] Dypvik and Bland,[10] investigating the connectivity of the RN with subcortical regions, pointed out that the neural activity of the RN in rats was also functionally related to the neural activity of hippocampal formation.

In primates, the 2 neuronal RN populations have the aforementioned subdivisions (RNm and RNp) and connections.[6,9,11,12] In rats[13,14] and opossums,[15] the RN is not so sharply subdivided into magnocellular and parvicellular regions, whereas in cats, not only are the magnocellular and parvicellular elements intermixed throughout the RN, but also the parvicellular population projects to the cervical spinal cord.[5] At present, little is known about the morphology, cytoarchitecture, and projections of the RN in cattle.

It is known that the pars intermedia of the lobus rostralis of the cerebellum exerts an inhibitory influence primarily over portions of the cerebellar nuclei interpositi; these nuclei, in turn, influence the contralateral thalamus and, in much lesser amounts, the contralateral RN, which influences the overlying motor cortex that then influences the motor activity via the corticospinal tract. In some mammals, such as cattle, the corticospinal tract is not well developed, and the cortico-rubro-spinal tract represents the main motor pathway.

Received March 23, 2006.
Accepted May 15, 2006.
From the Department of Veterinary Morphophysiology and Animal Productions (Chiocchetti, Bombardi, Grandis, Mazzuoli, Lucchi) and the Veterinary Clinical Department (Gentile, Pisoni, Joechler), University of Bologna, 40064 Ozzano dell'Emilia, Bologna, Italy.
Supported by the Region of Emilia-Romagna and the Ricerca Fondamentale Orientata (RFO, University of Bologna) grants.
Address correspondence to Dr. Chiocchetti.

Spinal cord RN terminations in monkeys and cats directly reach the motoneuronal pools (Rexed lamina IX), which innervate the muscles that move the digits.[16–19] This suggests that an RN disturbance could also be the basis of the pathogenesis of the spastic syndrome (ie, standing disease) of adult cattle[20] or BSP (ie, Elso Heel) of young calves,[21] characterized by hyperextension and spastic movements of the hind limbs. An RN disturbance may also be closely related to the subacute transmissible spongiform encephalopathies,[22,23] in which several neurotransmitter systems (the serotoninergic system in particular) are damaged.[24] It is suggested that the pathogenesis of BSP consists of a deterioration of a group of 5-hydroxytryptamine neurons at the mesencephalic level, mainly in the RN. In particular, the ruminant brainstem manifests the prion disease bovine spongiform encephalopathy. Recently, Miyashita et al[25] showed, by means of immunohistochemistry, a reduction of synaptophysin staining in the RN of cattle with bovine spongiform encephalopathy.

Our preliminary results have shown that in BSP-affected calves, the RN neurons projecting to the L6-S1 spinal cord segments seem to be considerably fewer and smaller than in control calves.[a] All these conditions of cattle are largely a motor neuron disease in nature, and better knowledge of motor pathways in large ruminants may lead to a better understanding of these disease processes.

The purpose of the study reported here was to elucidate the morphology, cytoarchitecture, and topographic organization of the RN with regard to its lumbosacral projections in cattle. The RN neurons sending their processes to the L6-S1 spinal cord segments were localized by use of retrograde axonal transport of the fluorescent tracer FB, and quantification and morphometric analysis of these FB-labeled neurons were performed.

Materials and Methods

Animals—Four young male Friesian calves weighing approximately 70 kg with an approximate age of 2 months were used in the study. Calves were maintained on a diet of hay and water ad libitum for 1 week before the experiment. Before surgery, calves were kept without food for 6 hours but were not deprived of water before anesthesia to avoid hypoglycemia. The University of Bologna Animal Experimentation Ethics Committee approved all procedures.

Surgical procedures—Tranquilization was performed by the administration of atropine sulfate (0.04 mg/kg, IM) and xylazine hydrochloride (0.22 mg/kg, IM). After recumbency and venous catheterization, induction of anesthesia was achieved by a rapid injection of thiopental sodium (8 to 15 mg/kg, IV). Endotracheal intubation was performed while calves were in sternal recumbency by use of laryngoscopy. An orogastric tube was also passed to promptly decompress the rumen and to allow the emission of the continuous gas formed, thereby avoiding ruminal meteorism. Anesthesia was maintained by mechanical ventilation with 1.5% to 2.0% isoflurane in oxygen. Supportive fluids were administered IV. Butorphanol tartrate (0.02 mg/kg, IV) was administered, and monitoring of pulmonary and cardiovascular function was performed at 5-minute intervals to maximize the safety of anesthesia and improve the likelihood of an uneventful recovery. During the recovery period, analgesia was achieved by the administration of ketoprofen (3 mg/kg, IM), and vital signs were continually monitored until the return of coughing, swallowing, and righting reflexes.

For surgery, calves were positioned in sternal recumbency and underwent dorsal laminectomy on L5. The skin incision was made on the midline, and the subcutaneous tissues were gently dissected from medial to lateral to reveal the muscular fascia. The lumbodorsal fascia was incised from L4 to L6 around and between the spinous processes. The longissimus lumborum muscle was bilaterally elevated, and this exposure was maintained by use of self-retaining Gelpi retractors. Because the spinous process of L5 had been revealed, the supraspinous ligament (ligamentum supraspinale) over L4-L5 and L5-L6 and the interspinous ligament between L4-L5 and between L5-L6 were incised. Therefore, the lamina was revealed, making it possible to remove the bone of the lamina and spinous process with rongeurs. When the laminectomy was performed, the spinal cord was revealed. Then a dorsal median durotomy was performed to better reveal the spinal cord fibers and roots. After fluorescent tracer injections, the dura was closed with tacking sutures, and muscles, fascia, and skin were closed by use of routine procedures.

Injection of fluorescent tracer—The exposed lumbosacral portion of the spinal cord was slowly infiltrated with multiple-site injections of the fluorescent tracer FB[b] (2% aqueous solution) by use of 10-µL Hamilton syringes. The fluo-

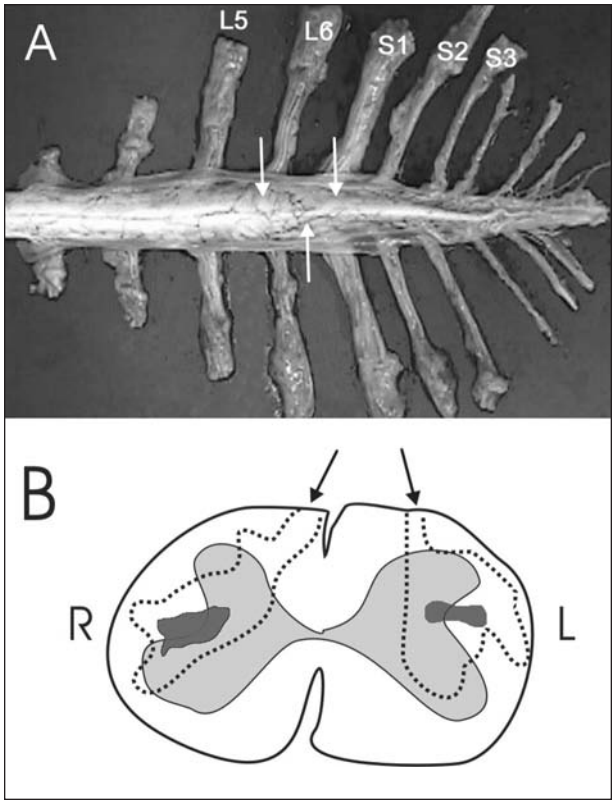

Figure 1—Photograph of the spinal cord (A) and drawing of L6 spinal cord section (B) of a calf injected with retrograde fluorescent tracer FB after L5 laminectomy. Notice the injection sites (white arrows) of dye at the L6-S1 spinal cord segments, port of entry of the needle (black arrows) through the dorsal surface of the spinal cord, and FB infiltrations (dotted lines). Local tissue destruction (dark gray areas) was related to needle insertion and application of the tracer. The purpose was to inject the fluorescent retrograde tracer into the lateral funiculi and in the dorsal horns of the gray matter. Tracer was also visible in the ventral horns of the gray matter. R = Right. L = Left.

rescent tracer produces a blue fluorescent labeling of the cytoplasm at an excitation wavelength of 360 nm. Injections were given at the L5 vertebral body (ie, at the L6-S1 spinal cord segments [caudal to the lumbar enlargement]; **Figure 1**).

Eight bilateral injections of FB (80 μL) were administered into the spinal cord, lateral to the midline, with the aim of injecting the rubrospinal tracts of both sides located in the lateral funiculi and the spinal cord where the lateral funiculi terminate; no attempts were made to produce unilateral injections of FB. To avoid a massive disruption of the spinal cord and the consequent paresis of the recovered calves, injections were distributed over a wide spinal cord area, cov-

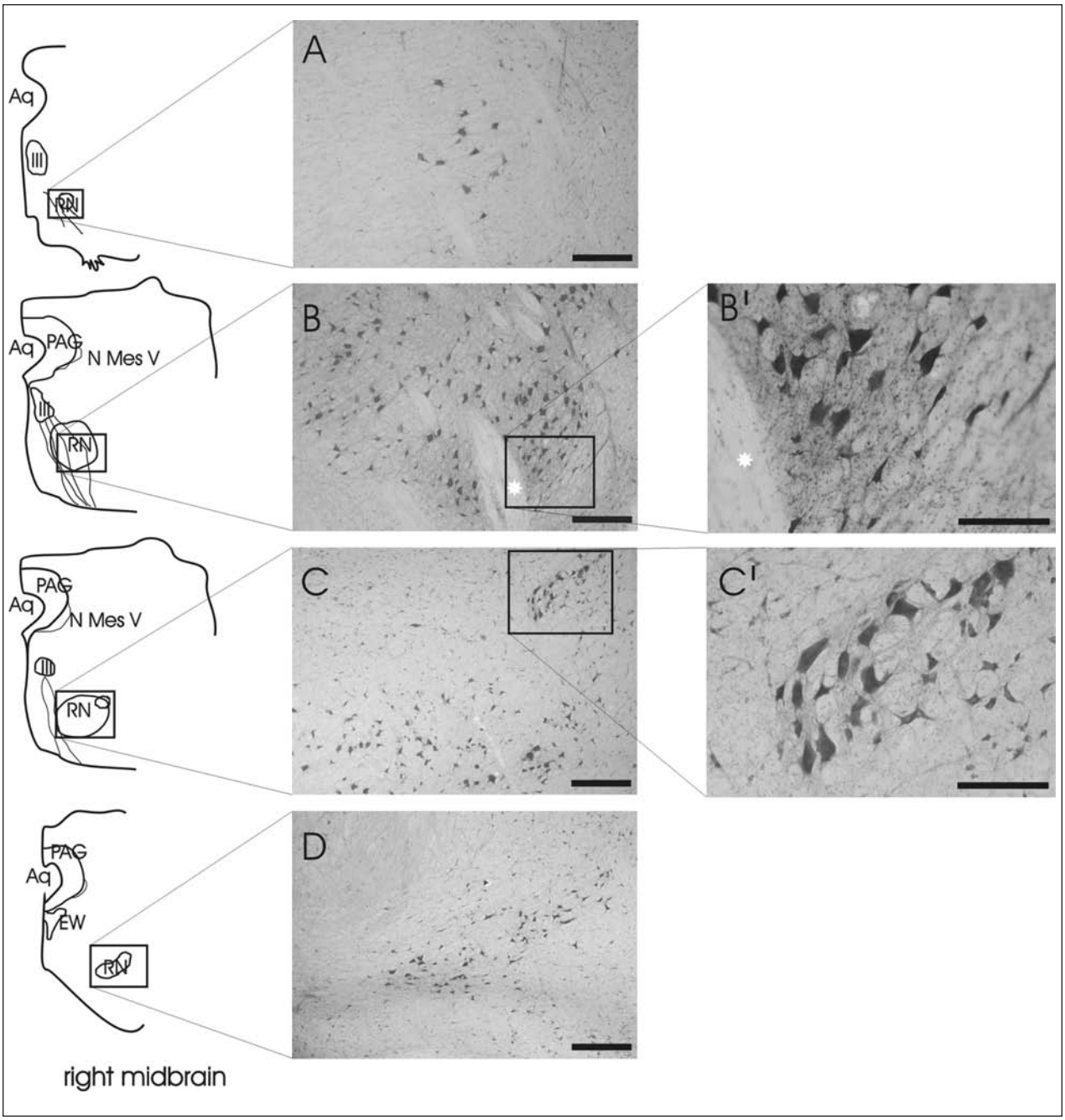

Figure 2—Sequence of drawings from photomicrographs (A through D) of Nissl-stained sections of the right RN from a calf. The RN was represented by a large column of neurons extending in the tegmentum of the midbrain caudally from the oculomotor fibers that cross the RN for approximately 4,000 μm cranially to the subthalamic region. Notice the caudal round end of the RN (panel A), composed of 4 to 12 multipolar large neurons. The RN at its maximum width (panel B; approx 1,200 μm cranially from its caudal end) has 2 groups of cells, 1 group of loosely arranged neurons located in central and dorsal positions, and 1 group of more densely packed neurons, ventrally located, mainly composed of small and medium cells. Notice the spindle neurons located on the ventral RN border (panel B'). Approximately 2,000 μm cranially from its caudal end (and visible for another 2,000 μm), the dorsolateral RN cluster (panel C) is found. Notice the dorsolateral cluster composed mainly of medium and large cells (panel C'). At the cranial end of the RN, where the mesencephalon joins the diencephalon, the loosely arranged neurons form a crescent like cluster that opened dorsomedially (panel D). All panels, Nissl's method of staining; panels A through D, bars = 500 μm; panels B' and C', bars = 200 μm. Asterisk= Oculomotor fibers crossing RN. Aq = Aqueduct of the mesencephalon. III = Oculomotor nucleus. PAG = Periaqueductal gray matter. N Mes V = Mesencephalic nucleus of the trigeminal nerve. EW = Edinger-Westphal nucleus (parasympathetic nucleus of oculomotor nerve).

ering the cranial end of L6 and caudal end of S1 spinal cord segments. Moreover, spaced injections had the possibility of maximizing the number of labeled RN neurons, as a single rubrospinal fiber can terminate along several segments of the spinal cord.[26] The syringe was gently withdrawn, and any tracer leakage was promptly removed from the surface of the spinal cord by means of a surgical aspirator. Although it was difficult to avoid partial inflammation of the injected spinal cord segments, all calves began to walk 1 to 2 days after surgery.

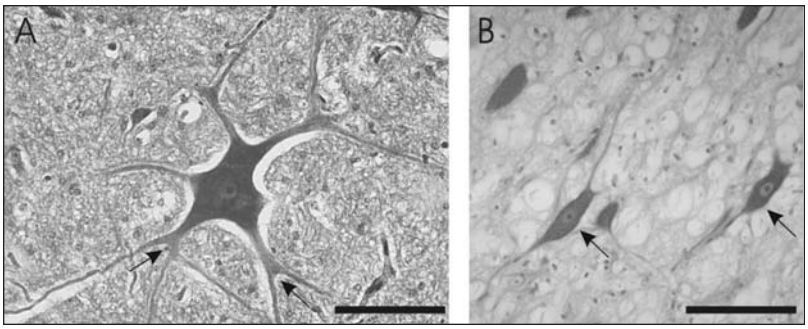

Figure 3—Photomicrographs of Nissl-stained sections of the RN from a calf, illustrating magnocellular and parvicellular RN cells. The paraffin-embedded section (15 µm thick; panel A) of a large multipolar neuron contains a centrally located nucleus with 5 large processes that bifurcate into 2 or more narrower elongated daughter branches (arrows). The cryostat section (60 µm thick; panel B) has 2 forked small neurons (arrows), as are often observed in the ventral border of the RN. Nissl's method of staining; bars = 100 µm.

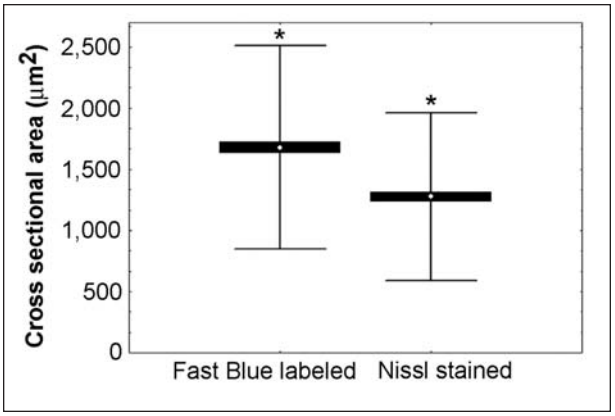

Figure 4—Box-and-whisker plots of mean cross-sectional areas of 300 FB-labeled and 300 Nissl-stained RN neurons that send their fibers to the caudal portion of the spinal cord (n = 3 calves). *Significant ($P < 0.05$) difference between FB-labeled and Nissl-stained RN neurons. Whiskers = SD. Box = SE. Open symbol = Mean.

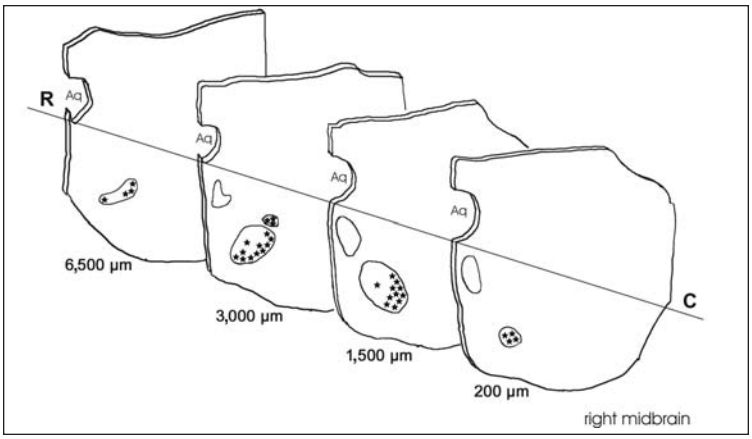

Figure 5—Schematic drawing illustrating the caudocranial distribution in the RN of FB-labeled neurons after injection of the tracer into the L6-S1 spinal cord segments. Distances from the caudal origin of the RN are indicated. The number of stars does not reflect the exact number of cells seen; rather, they indicate the relative density in the different levels of the RN. C = Caudal. R = Cranial (rostral). *See* Figure 2 for remainder of key.

Survival time—The appropriate calf survival time for the labeling of the RN neurons at the transport distance (85 to 95 cm) was determined by considering our own experience with this dye. For this study, a calf survival time of 38 to 55 days was used.

Tissue preparation—These procedures have been described elsewhere.[27] Briefly, at the end of the chosen survival time, calves were deeply anesthetized with thiopental sodium (15 mg/kg, IV) and euthanatized by means of IV administration of embutramide, mebenzonium iodide, and tetracaine hydrochloride. After euthanasia, the brain (encephalon) and the lumbosacral portion of the spinal cord were immediately exposed. After removal of the midbrain and the L5-S2 spinal cord segments, tissues were rapidly removed and immersion fixed for 48 to 72 hours in 4% paraformaldehyde in phosphate buffer (0.1M; pH, 7.2) at 4°C, rinsed overnight in PBS solution (0.15M NaCl in 0.01M sodium phosphate buffer; pH, 7.2), and stored at 4°C in PBS solution containing 30% sucrose and sodium azide (0.1%). Serial transverse sections of the spinal cord and midbrain sections (60 µm in thickness starting from the caudal surface of the specimens) were cut on a freezing microtome and mounted on uncoated slides, immediately dried with a warm air current and cover slipped with a mounting medium. Sections were observed with a microscope[e] equipped with a filter system[d] providing excitation light having a wavelength of 360 nm, which elicits the blue FB fluorescent labeling of the neuronal cytoplasm. The distribution of retrograde-labeled cells within the RN was charted with an XY plotter attached to the microscope stage by means of transducers.

In addition, midbrains of 4 additional calves were used. The material was fixed in Bouin's solution, embedded in paraffin, transversally and serially sectioned at a thickness of 15 µm, and stained according to the Nissl's method. Nissl's method was also used for staining some cryostat sections that had been analyzed previously for FB fluorescence.

Images were recorded by use of a digital camera[e] and a software program.[f] Contrast and sensitivity adjustment were performed with software programs.[g,h] Another software[i] program was used for the morphometric analysis of FB-labeled and Nissl-stained nerve cells throughout the RN; the somatic cross-sectional area of labeled neurons was measured after manual tracing of the cell outline. Three hundred FB-labeled RN neurons (from 3 calves) were measured. Three hundred Nissl-stained neurons (from 3 calves) were measured; sections at the caudal (1 section), central (2 sections), and cranial (1 section) portions of the RN were analyzed.

Statistical analysis—A sign test was used to evaluate the differences between the size of Nissl-stained and FB-labeled neurons. To evaluate the difference between the size of RNm and RNp neurons innervating the caudal portion of the spinal cord, the Student *t* test was used. A value of $P < 0.05$ was considered significant.

Results

Injection sites—The center of the injection sites characteristically had evidence of local tissue destruction relating to needle insertion and application of FB. Injection sites were identified within the L6-S1 spinal cord segments as areas with a large number of labeled neurons belonging to the ventral and dorsal horns of gray matter (Figure 1).

Nissl-stained RN morphology and cytoarchitecture—The RN of calves had a large column of neurons extending in the tegmentum of the midbrain caudally from the oculomotor fibers to the subthalamic region. The length of the RN from the caudal end to cranial end ranged from 6,680 to 8,640 µm (mean ± SD, 7,640 ± 853 µm). The caudal end of the RN was composed of 4 to 12 neurons (**Figure 2**), was round in shape, and was crossed dorsoventrally by the thick bundles of the oculomotor fibers, which were seen crossing the RN for approximately 4,000 µm cranially.

The maximum width (approx 4 mm) of the RN was located approximately 1,200 µm cranially from its caudal end. At this level, the RN was irregular or oval with its long axis ventrolaterally oriented and contained 2 groups of cells as follows: 1 large group, mainly composed of medium and large loosely grouped multipolar neurons located in the dorsal and central portions of the RN, and 1 smaller ventrally located and more densely packed group, mainly composed of small and medium cells. Fusiform small neurons were mainly observed ventrally to multipolar neurons.

The long axis of the RN was transversally oriented (or with a slight dorsolateral orientation) at approximately 2,000 µm (4,000 µm in 1 calf) cranially from its caudal end. At this level, a

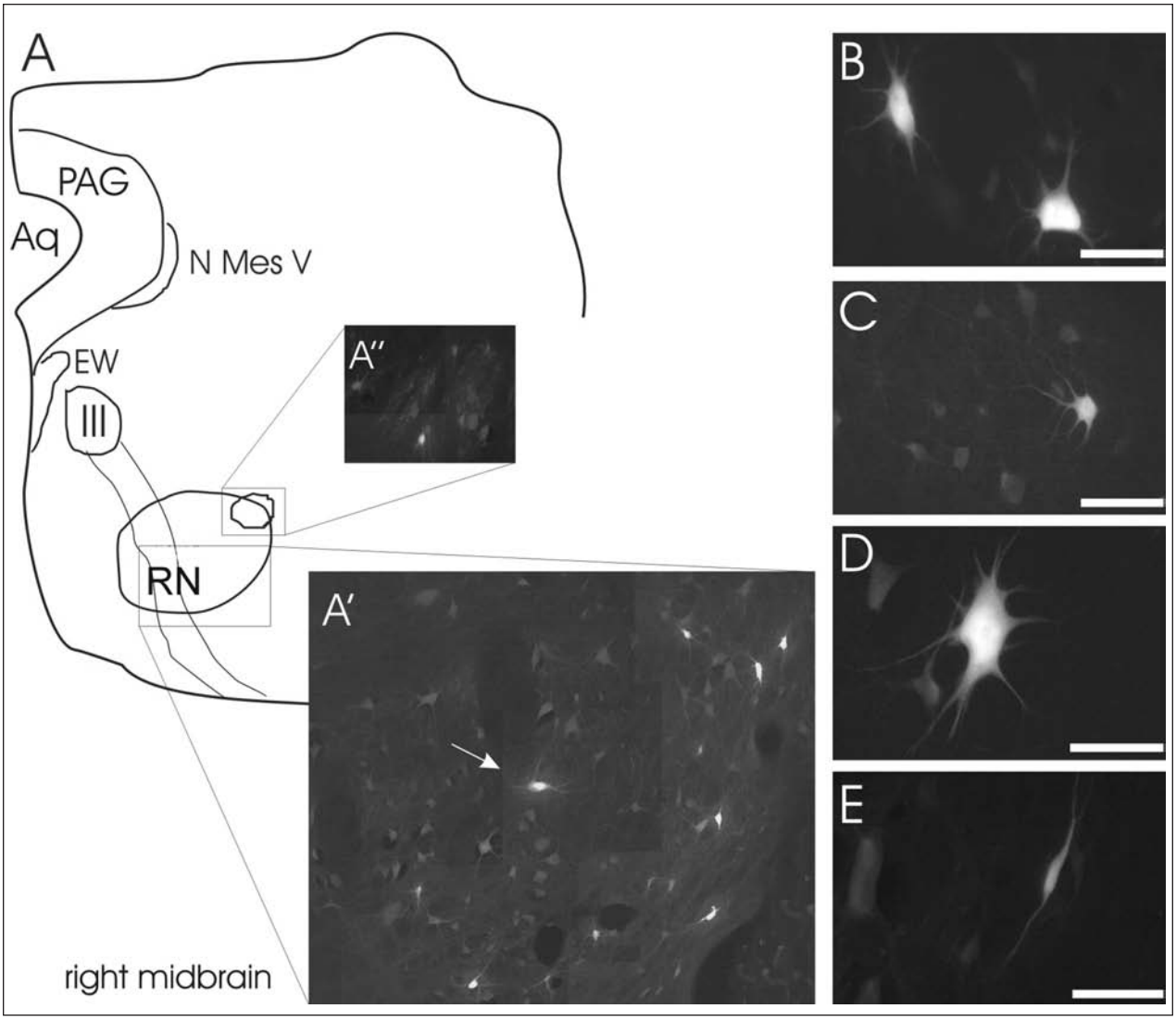

Figure 6—Drawing (panel A) of RN neuron distribution and photomicrographs (A', A'', and B through E) of sections of RN neurons that were labeled after injections of the retrograde FB tracer in the L6-S1 spinal cord segments of a calf. Notice the distribution of FB-labeled cells within the RN (panels A and A') and the dorsolateral cluster (panel A''); FB-labeled cells were confined to the ventrolateral part of the nucleus, but a few neurons were also visible in its central portion (arrow; panel A'). Two large multipolar FB-labeled neurons (panel B) belonged to the dorsolateral cluster. Notice the bright FB labeling of a multipolar neuron (panel C). The largest multipolar FB-labeled cells (panel D) had up to 10 broad emanating processes. Parvicellular bipolar neurons (panel E) were often visible in the ventral border of the nucleus. Panel B, bar = 50 µm; panel C, bar = 200 µm; panels D and E, bar = 100 µm. *See* Figure 2 for key.

cluster of neurons was observed dorsolaterally and prevalently composed of medium and large cells (Figure 2); it was visible for approximately 2,000 µm cranially. The shape of the RN was not easily recognizable at its cranial end, where the mesencephalon joins the diencephalon, and the neurons observed were smaller and loosely arranged, forming a crescentlike cluster that opened dorsomedially or were grouped in a cluster with a circular shape.

Analysis of the shape of 200 Nissl-stained neurons (from 1 calf) in 4 sections at different levels through the RN **(Figure 3)** revealed that cells were multipolar (122/200 [61%]), bipolar (34/200 [17%]), triangular (28/200 [14%]), and forked (16/200 [8%]). In 15-µm-thick sections, the multipolar neurons had up to 5 large processes emanating from them. Nuclei with large nucleoli were generally located in the middle of perikarya.

Nissl-stained RN neuron size—The mean ± SD cross-sectional area of 300 Nissl-stained cell bodies measured from 3 calves was 1,276 ± 686 µm^2 **(Figure 4)**. Cell bodies had cross-sectional areas that ranged from 205 and 4,073 µm^2. Only a few large cells were observed; the percentage of cells that had a cross-sectional area > 2,000 µm^2 was 13% (39/300), whereas the main RN neuronal population had a cross-sectional area ranging from 500 to 1,500 µm^2.

FB-labeled RN distribution and morphology—The FB-labeled neurons were distributed almost throughout the entire length of the RN and were more numerous in its caudal portion **(Figure 5)**. Cranial ends of neurons were not FB labeled for approximately 100 µm in only 1 calf. The labeled cells were mainly confined to the ventrolateral part of the nucleus, but a few FB-labeled cells were visible in its central portion **(Figure 6)**. Labeled cells varied in size, and the large and small neurons were intermixed throughout the RN, but the former predominated at the caudal end of the nucleus and the latter at the cranial end with a gradual transition between.

In the dorsolateral cluster, lying approximately 2,000 µm cranially from its caudal end, as described for the Nissl-stained sections, a number of FB-labeled rubrospinal neurons were found, mainly of large dimension. The FB labeling, observed mainly in the large neurons (Figure 6), was visible for the entire length of the dorsolateral cluster.

Analysis of the shape of 100 FB-labeled neurons (Nissl-stained cells from the same sections were also analyzed) revealed that cells were multipolar (93/100 [93%]), triangular (3/100 [3%]), bipolar (2/100 [2%]), and forked (2/100 [2%]). The bipolar and forked FB-labeled neurons (mainly belonging to the RN parvicellular component) were mainly observed ventrally in the RN, bordering the reticular formation, and often had small dimensions (Figure 5). The largest multipolar neurons had up to 10 processes emanating from them. The main processes were often divided into 2 narrower elongated daughter branches. The longest FB-stained processes could be followed for ≥ 200 µm.

FB-labeled RN neuron size—Mean ± SD cross-sectional area of 300 FB-labeled somata measured from 3 calves was 1,677 ± 831 µm^2. In particular, data related to the 3 calves were 1,735 ± 955 µm^2, 1,765 ± 816 µm^2, and 1,530 ± 687 µm^2, respectively.

The FB-positive neurons from 1 calf (ie, the calf with a mean soma cross-sectional area of 1,735 ± 955 µm^2) had cross-sectional areas that ranged from 386 to 6,284 µm^2; only a few huge cells were observed (cross-sectional areas of 3,700 to 6,284 µm^2). The percentage of FB-labeled cells that had a cross-sectional area > 2,000 µm^2 was 33% (33/100), whereas the main RN neuronal population had cross-sectional areas that ranged from 500 to 3,000 µm^2. The FB-labeled somata with a major axis > 100 µm were only 3% (3/100) of the total neuronal population. Observation of the cross-sectional area of FB-labeled somata throughout the RN caudocranial extension revealed that the caudal half of the RN was the largest FB-labeled somata (mean cross-sectional area, 1,940 µm^2) and that in the middle to cranial portion, the cellular area decreased (mean cross-sectional area, 1,460 µm^2). Evaluation of the size differences between RNm (multipolar and triangular) and RNp (bipolar and forked) FB-labeled neurons innervating the caudal portion of the spinal cord revealed that FB-labeled multipolar and triangular cells were significantly larger than forked and bipolar FB-labeled neurons.

Number of FB-labeled RN neurons—Labeled cells were included if a clearly identifiable nucleus could be discerned within the soma or at least 2 processes could be identified to branch from a clearly defined soma. The number of FB-labeled neurons ranged from 191 to 1,469 (mean, 465). In a calf that had 1,469 FB-labeled neurons throughout its length (7,260 mm), 10 to 16 FB-labeled neurons/section were observed approximately 800 mm cranially from the RN caudal end; 30 to 35 FB-labeled neurons/section were counted approximately 1,800 mm cranially from the caudal end of the RN. The cellular FB labeling was constant for an additional 2,600 mm (14 to 37 FB-labeled neurons/section) and then decreased in the next 1,300 mm (7 to 21 FB-labeled neurons/section). In the most cranial part of the RN (1,560 mm in length), 1 to 13 FB-labeled neurons/section were visible.

Discussion

Our study on cattle was focused on the morphology and cytoarchitecture of the RN and the distribution and somatotopic organization of RN neurons projecting to the caudal portion of the spinal cord levels (ie, to the L6-S1 spinal cord segments). Because total decussation of the rubrospinal tract has been found in all species studied in the past,[28] our study included bilateral spinal cord injections of the tracer so that we could investigate the right and left RN spinal cord projections in all calves. Nevertheless, a few investigators described a small uncrossed component of the rubrospinal fibers in monkeys,[J] rats,[29,30] and cats.[31] However in a recent study by Burman et al,[9] no uncrossed rubrospinal fibers were observed in monkeys.

The RN of calves described in our study is quite similar to the RN described by all investigators of the

mammalian brainstem.[1–6,32] However, we did not observe the traditional RN magnocellular division, made up almost exclusively of large neurons (caudal portion), and parvicellular division, made up of medium and small cells (cranial portion). In our study, small, medium, and large neurons were intermingled throughout the entire length of the RN and were loosely arranged only in its cranial end. Neurons of the central and caudal portions were organized loosely in a large dorsal group and in a smaller ventral compact cluster. Moreover, we observed another group of neurons clustered dorsolaterally to the RN column in the middle to caudal third of the RN. This cluster was also described in rabbits by Mahaim[33] and in cats.[1,5,34–37] Berman[38] did not describe this nucleus in the brain stem of cats; Mahaim[33] called this lateral small cluster the nucleus minimus. A dorsal group of medium rubrospinal neurons overlapping the cranial end of the RNm was also observed in monkeys[12]; Burman et al[9] named this cluster of RN neurons in monkeys the dorsolateral zone, which is composed of rubrospinal neurons that do not receive cortical input. In our study, bipolar FB-labeled neurons were observed, but it is possible that other spinal cord projections were present but not visible.

In our study, a significant difference was found between the mean cross-sectional areas of FB-labeled and Nissl-stained neurons. It is likely that the technical procedure (with ethanol and xylene) necessary for paraffin embedding and also for cell staining by use of Nissl's method does result in some shrinkage of tissues. Thus, with the aim to restrict tissue shrinkage and therefore to avoid larger error in evaluation of the cross-sectional areas of Nissl-stained RN neurons, the same section (from 3 calves) used for observation of FB-labeled neurons was also used for evaluation of Nissl-stained neurons. However, results of our study indicate that mainly large neurons project to the caudal portion of the spinal cord. Although the smaller neurons are probably involved in many other neuronal pathways (eg, rubrospinal tract for the thoracic limbs, ipsilateral nucleus olivaris, and interneurons), they also, as shown in cats by Pong et al,[5] send their processes to the caudal portion of the spinal cord.

In cats, which use limbs and feet for a wide variety of functions, the number of rubrospinal neurons belonging to the RNm has been roughly estimated to be approximately 450[39] or 2,000.[40] The number of FB-labeled cells observed in our study ranged from 191 to 1,469 (mean, 465). An unpredictable discontinuity was found in the number of FB-labeled cells observed. Several factors could account for this discrepancy. First, although every effort was made to inject the spinal cord at the same levels in all calves, it is possible that this was not accomplished and that the FB-fluorescent dye was much more concentrated in deeper spinal cord levels. Second, it is also possible that many FB-labeled RN neurons may have contained an undetectable amount of labeling material. Nevertheless, the great number of FB-labeled neurons detected in our study indicates that in cattle, as in other species, rubrospinal projections could play an important role in controlling limbs and digit movements.

In cattle, we observed that RNm and RNp populations send fibers to the spinal cord at the lumbosacral level. The extension of the rubrospinal projection does not differ from data obtained for rats, cats, and monkeys,[5,9,41–43] but some differences are found concerning the spinal cord projections of the RNp. In fact, the RNp of cats sends fibers that reach only the cervical level.[5] In monkeys, RNp does not project to the spinal cord but only to the nucleus olivaris.[9,42,43] Moreover, in our study, cells belonging to the so-called dorsolateral zone were FB-labeled cells, which are considered not to receive cortical input in monkeys.[9] Thus, it is hypothesized (by analogy) that a direct rubrospinal pathway, not only an indirect cortico-rubro-spinal pathway, is present in cattle.

Findings in our study help to define one of the main descending supraspinal projections to the lumbosacral portion of the spinal cord in cattle. Our study was concentrated on lumbar enlargement because of the functional importance of these spinal cord levels for hind limb movement. Our interest lies in the region of the L6-S1 spinal cord segments because this is the site where 2 important motoneuronal pools innervating the gastrocnemius and flexor digitorum superficialis muscles are located.[27] These 2 muscles are directly involved in one of the most widespread diseases in cattle, BSP. Pathogenesis of BSP is not completely understood, but an overactive stretch reflex resulting from an upper motor neuron alteration may be the basis of spastic paresis. It has been shown in cats that destruction of the RN causes little, if any, paresis of the limbs, leaving cats capable of standing and walking; instead, other kinds of motor abnormalities such as a mild increase of extensor tonus, deficiencies in placing, and hopping reactions and slight ataxia have been observed.[44,45]

Results of our study provide anatomic descriptions of the RN of cattle and a detailed mapping of its connections with the caudal portion of the spinal cord. Quantitative neuroanatomic analysis on rubrospinal projections descending to the L6-S1 spinal cord segments could also be useful for investigation of the rubrospinal control of the motor behavior of the pelvis and tail; tail movement is closely linked to the performance of the hind limbs and trunk in many activities, such as standing, locomotion, defense, micturition, defecation, and mating.[41]

a. Chiocchetti R, Grandis A, Bombardi C, et al. Proiezioni mediullo-ponto-mesencefaliche dirette al midollo spinale lombosacrale nel bovino sano e affetto da paresi spastica: indagine comparativa (abstr), in *Proceedings*. 59th Convengo Nazionale Societa Italiana Scienze Veterinarie SIS Vet 2005;99–100.
b. Sigma-Aldrich Chemie, Steinheim, Germany.
c. Axioplan epifluorescence microscope, Carl Zeiss, Oberkochen, Germany.
d. Filter system A, Carl Zeiss, Oberkochen, Germany.
e. DMC, Polaroid Corp, Cambridge, Mass.
f. DMC2, Polaroid Corp, Cambridge, Mass.
g. Corel photo paint, Ottawa, ON, Canada.
h. Corel draw, Ottawa, ON, Canada.
i. KS300 Zeiss, Kontron Elektronik, Munich, Germany.
j. Bodian D. Spinal projections of brainstem in rhesus monkey deduced from retrograde chromatolysis (abstr). *Anat Rec* 1946;94:512–513.

References

1. Davenport HA, Ranson SW. The red nucleus and the adjacent cell groups. A topographic study in the cat and in the rabbit. *Arch Neurol Psychiatr* [Chicago] 1930;24:257–266.

2. Pompeiano O, Brodal A. Experimental demonstration of a somatotopical origin of rubrospinal fibres in the cat. *J Comp Neurol* 1957;108:225–250.

3. Flumerfelt BA, Otabe S, Courville J. Distinct projections to the red nucleus from the dentate and interposed nuclei in the monkey. *Brain Res* 1973;50:408–414.

4. Huisman AM, Kuypers HG, Verburg CA. Differences in collateralization of the descending spinal pathways from red nucleus and other brain stem cell groups in cat and monkey. *Prog Brain Res* 1982;57:185–217.

5. Pong M, Horn KM, Gibson AR. Spinal projections of the cat parvicellular red nucleus. J Neurophysiol 2002;87:453–468.

6. Massion J. The mammalian red nucleus. *Physiol Rev* 1967;47:383–424.

7. Sarkisian VH, Fanardjian VV. Antidromic and synaptic activation of Deiters' neurons induced by stimulation of red nucleus in the cat. *Neurosci Lett* 1992;136:47–50.

8. Bacskai T, Szekely G, Matesz C. Ascending and descending projections of the lateral vestibular nucleus in the rat. *Acta Biol Hung* 2002;53:7–21.

9. Burman K, Darian-Smith C, Darian-Smith I. Macaque red nucleus: origins of spinal and olivary projections and terminations of cortical imputs. *J Comp Neurol* 2000;423:179–196.

10. Dypvik AT, Bland BH. Functional connectivity between the red nucleus and the hippocampus supports the role of the hippocampal formation in sensorimotor integration. *J Neurophysiol* 2004;92:2040–2050.

11. King JS, Schwyn RC, Fox CA. The red nucleus in the monkey (*Macaca mulatta*): a Golgi and an electron microscope study. *J Comp Neuro*l 1971;142:75–108.

12. Kennedy PR, Gibson AR, Houk JC. Functional and anatomical differentiation between parvicellular and magnocellular regions of red nucleus in the monkey. *Brain Res* 1986;364:124–136.

13. Reid JM, Flumerfelt BA, Gwyn DG. An ultrastructural study of the red nucleus in the rat. *J Comp Neurol* 1975;162:363–385.

14. Reid JM, Gwyn DG, Flumerfelt BA. A cytoarchitectonic and Golgi study of the red nucleus in the rat. *J Comp Neurol* 1975;162:337–361.

15. King JS, Bowman MH, Martin GF. The red nucleus of the opossum (*Didelphis marsupialis virginiana*): a light and electron microscopy study. *J Comp Neurol* 1971;143:157–184.

16. Hongo T, Jankowska E, Lundberg A. The rubrospinal tract. I. Effects on alpha-motoneurons innervating hindlimb muscles in cats. *Exp Brain Res* 1969;7:344–364.

17. McCurdy ML, Hansma JC, Gibson AR. Selective projections from the cat red nucleus to digit motor neurons. *J Comp Neurol* 1987;265:367–379.

18. Holstege G, Blok BF, Ralston DD. Anatomical evidence for red nucleus projections to motoneuronal cell groups in the spinal cord of the monkey. *Neurosci Lett* 1988;95:97–101.

19. Ralston DD, Milroy AM, Holstege G. Ultrastructural evidence for direct monosynaptic rubrospinal connections to motoneurons in *Macaca mulatta*. *Neurosci Lett* 1988;95:102–106.

20. Wells GA, Hawkins SA, O'Toole DT, et al. Spastic syndrome in a Holstein bull: a histologic study. *Vet Pathol* 1987;24:345–353.

21. Roberts SJ. Hereditary spastic diseases affecting cattle in New York State. *Cornell Vet* 1965;55:637–644.

22. Ledoux JM. Bovine spastic paresis: etiological hypotheses. *Med Hypotheses* 2001;57:573–579.

23. Ledoux JM. Hypothesis of interference to superinfection between bovine spastic paresis and bovine spongiform encephalopathy; suggestions for experimentation, theoretical and practical interest. *Med Hypotheses* 2004;62:346–353.

24. Ledoux JM. Effects on the serotoninergic system in subacute transmissible spongiform encephalopathies: current data, hypotheses, suggestions for experimentation. Med Hypotheses 2005;64:910–918.

25. Miyashita M, Stierstorfer B, Schmahl W. Neuropathological findings in brains of Bavarian cattle clinically suspected of bovine spongiform encephalopathy. *J Vet Med B Infect Dis Vet Public Health* 2004;51:209–215.

26. Shinoda Y, Ghez C, Arnold A. Spinal branching of rubrospinal axons in the cat. *Exp Brain Res* 1977;30:203–218.

27. Chiocchetti R, Grandis A, Bombardi C, et al. Localization, morphology and immunohistochemistry of the efferent and afferent neurons innervating the gastrocnemius and the flexor digitorum superficialis muscles in cattle. *Am J Vet Res* 2005;66:710–720.

28. Strominger RN, McGiffen JE, Strominger NL. Morphometric and experimental studies of the red nucleus in the albino rat. Anat Rec 1987;219:420–428.

29. Shieh JY, Leong SK, Wong WC. Origin of the rubrospinal tract in neonatal, developing, and mature rats. *J Comp Neurol* 1983;214:79–86.

30. Antal M, Sholomenko GN, Moschovakis AK, et al. The termination pattern and postsynaptic targets of rubrospinal fibers in the rat spinal cord: a light and electron microscopic study. *J Comp Neurol* 1992;325:22–37.

31. Holstege G. Anatomical evidence for an ipsilateral rubrospinal pathway and for direct rubrospinal projections to motoneurons in the cat. *Neurosci Lett* 1987;74:269–274.

32. Castaldi L. Studi sulla struttura e sullo sviluppo del mesencefalo: Ricerche in *Cavia cobaya*. Parte 4. *Arch Ital Anat Embriol* 1928;25:157–306.

33. Mahaim A. Recherches sur la structure anatomique du noyau rouge et ses connexions avec le pédoncule cerébélléux supérieur. *Mém cour Acad r Méd Belg* 1894;13:1–44.

34. Monakov C von. Der rote Kern, die haube und die regiohypothalamica bei einigen Säugetieren und beim menschen. I. *Teil Arb hirnanat Inst Zürich* 1909;3:49–267.

35. Brown JO. The nuclear pattern of the non-tectal portion of the midbrain and isthmus in the dog and cat. *J Comp Neurol* 1943;78:365–405.

36. Brodal A, Gogstad AC. Rubro-cerebellar connections: an experimental study in the cat. *Anat Rec* 1954;118:455–485.

37. Taber E. The cytoarchitecture of the brain stem of the cat. I: brain stem nuclei of cat. *J Comp Neurol* 1961;116:27–69.

38. Berman AL. *The brain stem of the cat. A cytoarchitectonic atlas with stereotaxic coordinates*. Madison, Wis: University of Wisconsin Press, 1968;53.

39. Grofova I, Marsala J. Nucleus ruber kocky. *Morphologie* 1961;91:209–220.

40. Robinson FR, Houk JC, Gibson AR. Limb specific connections of the cat magnocellular red nucleus. *J Comp Neurol* 1987;257:553–577.

41. Masson RL Jr, Sparkes ML, Ritz LA. Descending projections to the rat sacrocaudal spinal cord. *J Comp Neurol* 1991;307:120–130.

42. Miller RA, Strominger NL. Efferent connections of the red nucleus in the brainstem and spinal cord of the rhesus monkey. *J Comp Neurol* 1973;152:327–346.

43. Carlton SM, Chung JM, Leonard RB, et al. Funicular trajectories of brainstem neurons projecting to the lumbar spinal cord in the monkey (*Macaca fascicularis*): a retrograde labeling study. *J Comp Neurol* 1985;241:382–404.

44. Ingram WR, Ranson SW. Effects of lesions in the red nucleus of cats. *Arch Neurol Psychiat* [Chicago] 1932;28:483–512.

45. Ingram WR, Ranson SW. The place of the red nucleus in the postural complex. *Am J Physiol* 1932b;102:466–475.